Nucl Eng Technol 47 (2015) 165–175

Available online at www.sciencedirect.com

ScienceDirect

journal homepage: http://www.journals.elsevier.com/nuclear-engineering-and-technology/

Original Article

STUDY OF CORE SUPPORT BARREL VIBRATION MONITORING USING EX-CORE NEUTRON NOISE ANALYSIS AND FUZZY LOGIC ALGORITHM

ROBBY CHRISTIAN [a], *SEON HO SONG* [b], *and HYUN GOOK KANG* [a,*]

[a] *Nuclear and Quantum Engineering Department, Korea Advanced Institute of Science and Technology, KAIST, 291 Daehak-ro (373-1 Guseong-dong), Yuseong-gu, Daejeon, 305-701, Republic of Korea*

[b] *Korea Institute of Nuclear Safety, 62 Gwahak-ro, Yuseong-gu, Daejeon, 305-338, Republic of Korea*

ARTICLE INFO

Article history:
Received 8 October 2014
Received in revised form
8 December 2014
Accepted 8 December 2014
Available online 21 January 2015

Keywords:
Fuzzy logic
Monte Carlo
Neutron noise analysis
Vibration monitoring

ABSTRACT

The application of neutron noise analysis (NNA) to the ex-core neutron detector signal for monitoring the vibration characteristics of a reactor core support barrel (CSB) was investigated.

Ex-core flux data were generated by using a nonanalog Monte Carlo neutron transport method in a simulated CSB model where the implicit capture and Russian roulette technique were utilized. First and third order beam and shell modes of CSB vibration were modeled based on parallel processing simulation. A NNA module was developed to analyze the ex-core flux data based on its time variation, normalized power spectral density, normalized cross-power spectral density, coherence, and phase differences. The data were then analyzed with a fuzzy logic module to determine the vibration characteristics.

The ex-core neutron signal fluctuation was directly proportional to the CSB's vibration observed at 8 Hz and 15 Hz in the beam mode vibration, and at 8 Hz in the shell mode vibration. The coherence result between flux pairs was unity at the vibration peak frequencies.

A distinct pattern of phase differences was observed for each of the vibration models. The developed fuzzy logic module demonstrated successful recognition of the vibration frequencies, modes, orders, directions, and phase differences within 0.4 ms for the beam and shell mode vibrations.

1. Introduction

To achieve a high level of safety while maintaining a high level of plant availability, it is desirable to perform preventive measures instead of corrective ones. One of these measures is the monitoring of reactor internals vibration characteristics. Any change in the vibration signatures may indicate an anomaly in the reactor internals. A significant structure to be

* *Corresponding author.*
E-mail address: hyungook@kaist.ac.kr (H.G. Kang).

http://dx.doi.org/10.1016/j.net.2014.10.002
1738-5733/Copyright © 2015, Published by Elsevier Korea LLC on behalf of Korean Nuclear Society.
Special Issue on ISOFIC/ISSNP2014.

monitored is the core support barrel (CSB). One method to monitor the CSB's vibration is by analyzing the neutron flux sensed by ex-core detectors around it as demonstrated by Yun et al [1].

A typical pressurized water reactor (PWR) core schematic is shown in Fig. 1. The CSB is fixed to the vessel at its top section. The high-pressure coolant's flow creates flow-induced vibrations in the CSB. To limit the vibrations' effects, mechanical snubbers are installed at the bottom part of the CSB.

Much research has been done to monitor the CSB's vibrations. Song and Jhung [2] utilized the analytical finite element model to calculate the CSB's frequency response function and validated it experimentally with a modal analysis experiment on a scaled-down model of the APR1400's CSB. The modal analysis was done by a shaker test using vibration sensors attached to the CSB model. Further research conducted by Ansari et al [3] correlated the ex-core detector data and vibration sensors mounted on reactor structure and control rod drive mechanisms. As a result they were able to identify a particular control rod that had a different vibration signature. They also concluded that the use of ex-core neutron noise analysis (NNA) was more sensitive in determining the dynamic behavior of reactor internals compared to the vibration sensors. Additionally, the ex-core NNA method can also be used to monitor the condition of thermal shield systems attached to the CSB [4]. This was done by analyzing the correlation of the vibration monitoring results with loose-part monitoring data as performed by Lubin et al [4] on the St Lucie PWR nuclear power plant. The CSB could also be modelled through a finite element approach and be monitored using neural networks [5].

Standards and guides have been written on the conduct of ex-core detector data analysis for vibration monitoring. The American Society of Mechanical Engineers (ASME) published two similar guides in the ASME OM-S/G-2007 document [6]. Part 5 of this document focuses on specifically monitoring the core support barrel axial preload. Part 23 elaborates on the monitoring of reactor internals vibrations in general. The United States Nuclear Regulatory Commission specifically issued Regulatory Guide 1.20 on The Comprehensive Vibration Assessment Program [7].

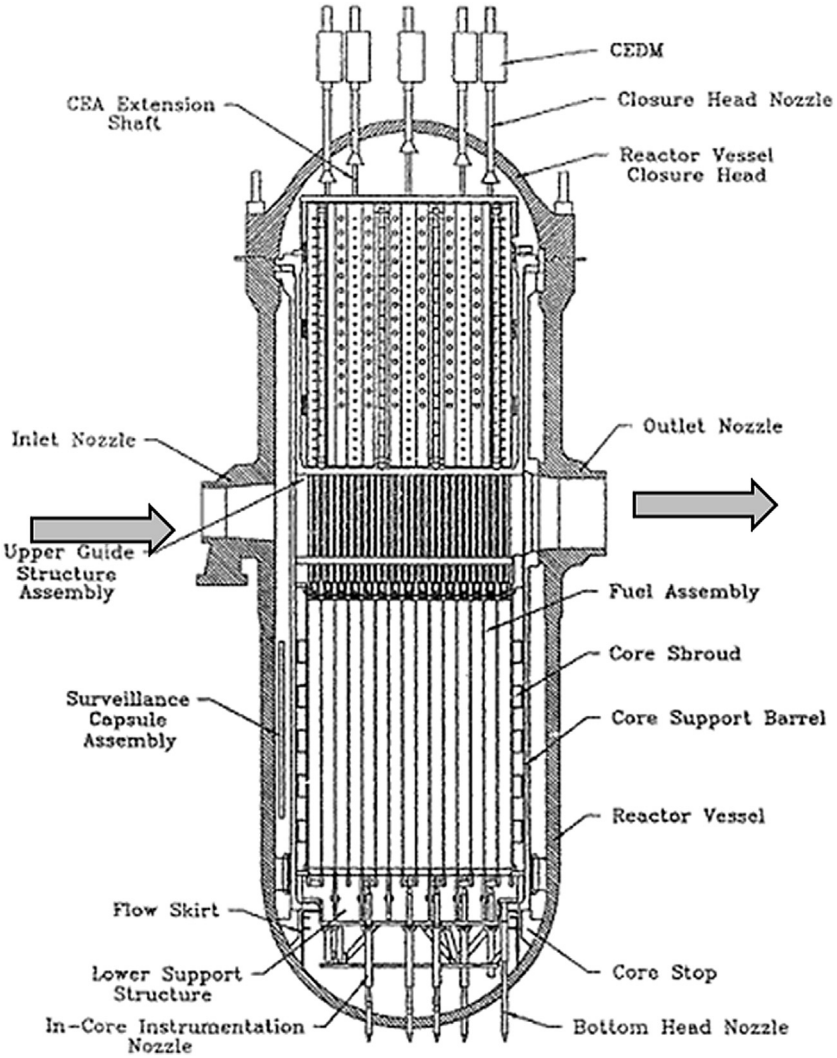

Fig. 1 – Pressurized water reactor core schematic.

This study aims to seek a practical implementation of ASME OM-S/G-2007 Part 5 and Part 23 to monitor flow induced vibrations on a CSB using ex-core neutron noise analysis. It revolves around finding how a CSB's vibration can affect the neutron flux outside of it, and how the neutron flux can be analyzed to extract information about the vibration of the CSB including its frequency, modes, and directions. Furthermore this study intends to improve the NNA to be able to analyze third order vibration modes. To achieve that, this study uses the Monte Carlo method to simulate neutron transport progressions in a vibrating cylindrical shielding. The vibrations considered here are beam mode and shell mode vibrations in their first and third order variants. A fuzzy logic recognition module was developed based on the observed pattern for faster identification of the vibration characteristics. This study does not address the monitoring of vibration amplitudes.

2. Materials and methods

2.1. *Monte Carlo neutron transport*

In the absence of measured ex-core neutron data, a simplified model of a neutron source inside a vibrating CSB was developed. Fig. 2 gives a general illustration of this model. The variables sampled for a three-dimensional flight in this case were the neutron's initial position h, azimuthal angle Φ, polar (elevation) angle θ, travel distance r, and the absorption instance shortly after the flight. Transformation from polar coordinates to Cartesian coordinates was done by trigonometric calculations.

Suppose that σ_A and σ_S are a neutron's absorption cross-section and scattering cross-section, respectively, in a certain medium. The total neutron removal cross-section σ_T is defined as:

$$\sigma_T = \sigma_S + \sigma_A \tag{1}$$

Neutron leakage from the core is typically limited due to the design objective to conserve the neutron economy. Therefore it will require a large number of simulation iterations to obtain ex-core flux data with a reasonably acceptable variance. Our study employed an implicit capture approach instead to reduce this variance without significantly increasing the random walk iterations. In the implicit capture method, the neutrons' absorption instance is replaced by a weight reduction scheme. Neutrons are initially given a weight value that decreases gradually as they travel within a medium under the following equation:

$$w_{(t)} = w_{(t-1)}\sigma_S/\sigma_T \tag{2}$$

When a neutron's weight is deemed trivial, it is eliminated from the simulation by the Russian roulette method [8]. In this method, two variables are determined, namely the weight threshold value and survival weight value. When a neutron's weight is less than the threshold value, a uniform random number is sampled. If this random number is greater than the ratio between the respective neutron's weight and the survival weight, the neutron is eliminated. If it is less, the neutron is assigned a new weight value based on the survival weight value. Survival weight is taken arbitrarily to be greater than the weight threshold value. A sensitivity study was performed on the fluxes' variance to select the optimal weight threshold value. This was done by running the simulation with varying weight threshold values in the range from 10^{-9} to 10^{-1}. A complete flowchart of the simulation is given in Fig. 3.

In this research, the 32-bit MT19937 variant of the Mersenne Twister algorithm was used as the pseudorandom number generator (PRNG). The parallel computing technique was used to speed up the Monte Carlo simulation. In a quad-core central processing unit, four processors perform the simulation in parallel. Each CSB discrete movement point was simulated in a processor, and the results were combined with results from other processors. For each parallel process, a different stream of MT19937 was generated and fed into it. To assure that each MT19937 stream meets the randomness criteria and is independent of other streams, first a time-seeded PRNG was created. After removing any consequent duplicate entries, this PRNG was then used to seed the MT19937.

The CSB and coolant were modelled as a solid cylindrical structure with uniform neutron absorption and scattering cross sections. A line-shaped neutron source was located at the center of the CSB, stretching from its top to the bottom plane. The selection of such a simple model was justified by the fact that the neutron noise analysis is conducted when the reactor is operating at a steady state. This structure was surrounded by neutron detectors having an assumed 100% efficiency spread across four quadrants. Two major modes of vibration were then simulated on the CSB. One was comprised of two simultaneous beam mode vibrations having frequencies of 8 Hz and 15 Hz. Another had a shell mode vibration at 8 Hz. For each of these vibration modes, the first and third order vibrations were introduced, having considered the clamped-pinned condition of the CSB. It was hypothesized that a group of four detectors would be sufficient to monitor the first order vibration due to the nature of the CSB's movement. However, for the third order vibration, it was necessary to separately monitor the movement of the CSB's upper and lower sections. Therefore two groups of four detectors each were used at different elevation levels. The sampling frequency was selected based on the Nyquist criteria. Schematic configurations of the system are given in Figs. 4 and 5.

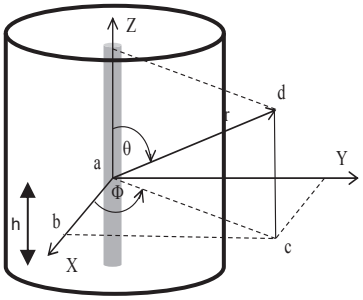

Fig. 2 – Polar coordinates for neutron transport.

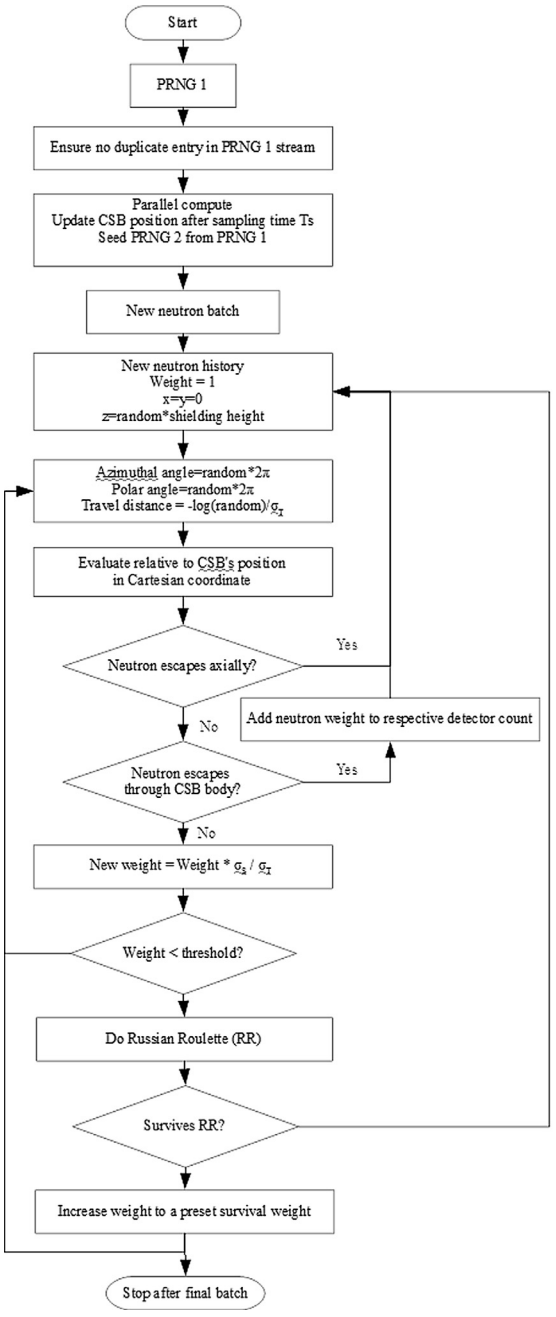

Fig. 3 – Monte Carlo simulation flow. CSB, core support barrel; PRNG, pseudorandom number generator.

2.2. NNA

On the assumption that ex-core neutron flux variations are caused only by the attenuation from the moderator, the following shielding equation applies [6]:

$$\varnothing_d = \varnothing_0 e^{-X\Sigma_r} \tag{3}$$

where X = shielding's thickness, $\varnothing_d$ = the attenuated neutron flux, $\varnothing_0$ = the incoming source flux, and Σ_r = the effective neutron removal cross-section.

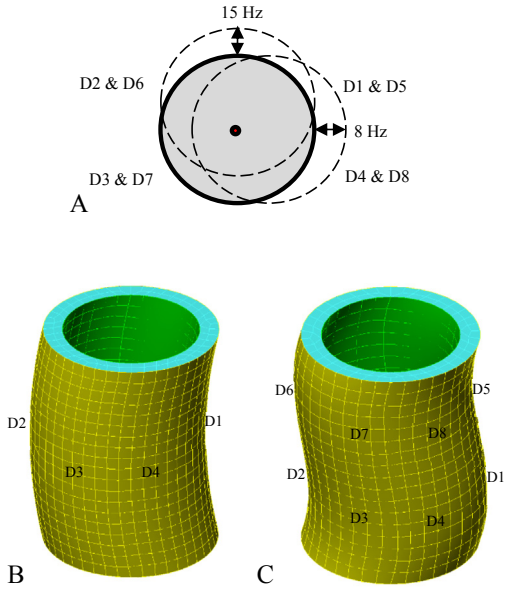

Fig. 4 – Beam mode vibration. (A) Core support barrel cross-section and vibrations. (B) First order. (C) Third order.

When the CSB vibrates it undergoes a translation after a certain time has elapsed. This process changes the thickness of the water gap by ΔX. Equation 3 then becomes:

$$\varnothing'_d = \varnothing_0 e^{-(X+\Delta X)\Sigma_r} \tag{4}$$

For dynamic measurements, the difference between $\varnothing_d$ and $\varnothing_0$ is the instantaneous neutron noise voltage such that it can be written as follows in the frequency domain:

$$\Delta X(\omega) = \frac{1}{\Sigma_r}\left[\frac{\Delta\varnothing(\omega)}{\varnothing_d}\right] \tag{5}$$

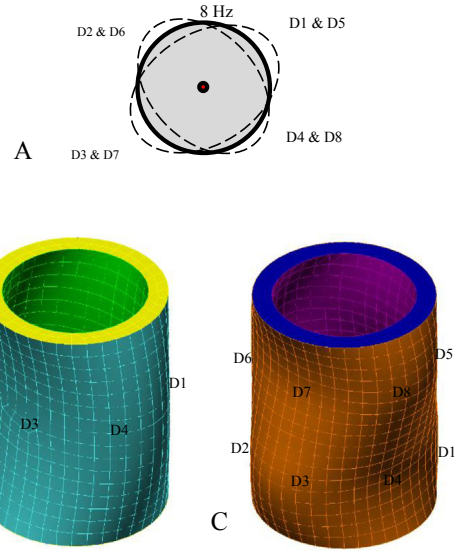

Fig. 5 – Shell mode vibration. (A) Core support barrel cross section and vibrations. (B) First order. (C) Third order.

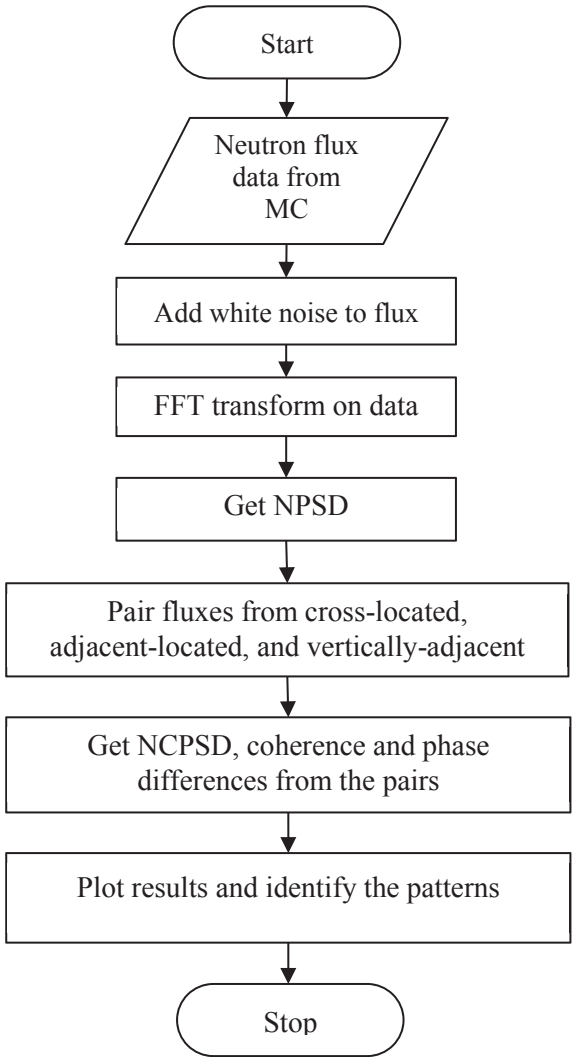

Fig. 6 – Neutron noise analysis flowchart. FFT, Fourier fast transform; MC, Monte Carlo; NCPSD, normalized cross power spectral density; NPSD: normalized power spectral density; PRNG: pseudorandom number generator.

The NNA flowchart is given in Fig. 6. A discrete white noise spectrum based on the central limit theorem was added to the neutron. Using MT19937 PRNG, 50 uniform random numbers were sampled, summed, and normalized for their DC level, and adjusted for variance to form the white noise spectrum. The justification for adding this white noise spectrum is elaborated upon in Section 5. The frequency domain data was extracted from the sequence of time series fluxes by using fast Fourier transformation (FFT) [9]. This FFT process generates the power spectral density (PSD) function. The PSD was then normalized to obtain the normalized power spectral density (NPSD) by dividing it by the square of the mean value voltage from the detector.

$$NPSD(\omega) = PSD(\omega) \Big/ \overline{\varnothing_d^2} \tag{6}$$

NPSD represents the frequency spectrum of a single flux. To analyze the frequency spectrum of two different fluxes, the normalized cross power spectral density (NCPSD) was used. NCPSD is obtained by cross-correlating two fluxes and performing FFT prior to dividing it by the product of the mean values from both fluxes.

Another variable was also used to represent the similarities between two spectrums. Coherence is defined as the ratio of the square of the magnitude of NCPSD to the product of individual NPSDs. Coherence has a value ranging between 0 and 1. For the neutron noise analysis, a coherence value above 0.5 is considered good enough to justify that the two signals are coherent. When this happens, the phase differences between the signals are valid.

$$Coherence = NCPSD_{xy} / (NPSD_x \times NPSD_y) \tag{7}$$

The phase angle of a spectrum is given as the arc tangent of the ratio between the spectrum's imaginary part and its real part:

$$\theta = \tan^{-1}(Im/Re) \tag{8}$$

2.3. *Fuzzy inference system*

It was noted that human errors in deciding the vibration's mode and directions could easily occur when manual examinations upon the NNA's signal were conducted. Furthermore, this process required a relatively long time to complete due to the noisy nature of the phase differences signal. These observations led to the development of an automated decision support system. This system is based on the fuzzy logic method in consideration of its simplicity and practicality. The signal pattern arising from the CSB's vibration is considered simple enough to be resolved by the fuzzy logic method. The use of fuzzy logic also eliminates the need for exhaustive training and learning periods required by some other alternative methods [10].

The fuzzy inference system (FIS) module was designed to analyze the NCPSD, coherence, and phase differences data in order to categorize the vibration characteristics. It is expected that the use of the FIS module may track vibration changes much faster than human analysis. The membership function for coherence is given in Fig. 7, while the membership function for phase differences is shown in Fig 8. A pair of flux spectra is considered coherent when their crisp value is >0.5. This flux pair is in phase when the crisp value is >0.5 around 0°, and out-of-phase when the crisp value is >0.5 around 180°.

A peak detection module was constructed and applied to the NCPSD signals. When a peak is detected, the system will

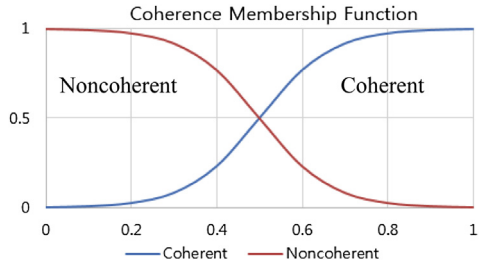

Fig. 7 – Coherence fuzzy membership function.

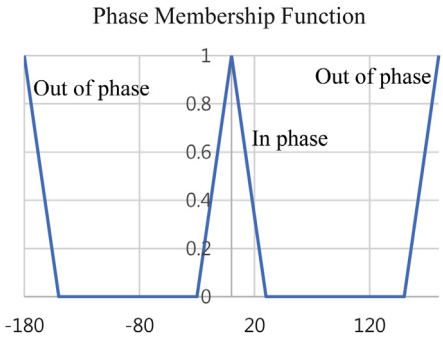

Fig. 8 – Phase difference membership function.

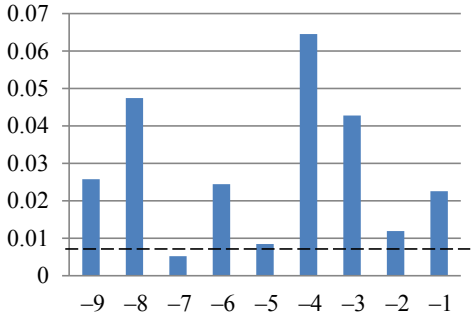

Fig. 9 – Sensitivity analysis result.

run the coherence FIS. If the signals are coherent, the phase FIS is executed. To detect a peak, first the NCPSD signal was transformed into its piecewise approximation to filter out noise. The statistical mode of this piecewise signal was then determined as the DC level. The signal was then scanned for local maxima having downward slopes on both of its sides.

Valid NCPSD peaks were checked for their coherence based on the membership function in Fig. 7. Coherent peaks were analyzed for their phase difference's state based on the function in Fig. 8.

Based on the NNA results, the combination of phase differences between flux pairs listed in Table 1 was used for the FIS results to determine the vibration mode in its first order, when a coherent NCPSD peak was detected. When a phase difference pattern in the table is found and the vertical detector pairs are out of phase then the vibration is of the third order instead.

3. Results and discussion

Fig. 9 shows the sensitivity analysis result on the effect of neutron weight threshold towards the variance of all detectors' variances. The x-axis is the logarithmic form of the weight threshold in the range from 10^{-9} to 10^{-1}. Based on this result, the neutron weight threshold was chosen to be 10^{-7} since it gave rise to the smallest spread of fluxes' variances. This implies that the neutron detectors' readings have closely related confidence levels in comparison to when another neutron weight threshold was used.

Results for the first order beam mode vibration analysis are shown in Fig. 10. The flux variation in the time domain (Fig. 10A) roughly shows two major vibration frequencies. This was confirmed in the frequency domain plot (Fig. 10B). The 8 Hz and 15 Hz peaks came from the common vibration source as shown by NCPSD (Fig. 10C). The flux pairs were coherent at these two peaks (Fig. 10D) and thus their phase differences were valid. However, another peak of 26 Hz also yielded a high coherence between the 2–4 and 3–4 flux pairs. This peak was ruled out because it was not detected in either NPSDs or NCPSDs, and because its value of 1.1 was above the coherence value range. This might be caused by the lack of a wide-spectrum noise signal which caused NPSD values at the nonpeak region to become very small and triggered the wrong result in the NCPSD calculation. By adding a white-noise spectrum to the time-flux data, the 26 Hz peak was eliminated (Fig. 10E).

At 8 Hz all the flux pairs were completely out of phase as seen in Fig. 10F. This was caused by the pattern of the CSB's movement. When the CSB moved towards Detector 1, it moved away from Detectors 2 and 3. The same explanation applies to the other detector pairs. This pattern originates from a beam mode vibration along the x-axis direction. At 15 Hz, the adjacent flux pairs were nearly in phase, whereas the opposite pairs were completely out of phase. When the CSB moved towards detector 1, it also moved in the same fashion towards Detector 2 yet away from Detector 3. This pattern is most likely to have originated from a beam mode CSB vibration along the y-axis direction as illustrated in Fig. 4A.

Results for the first order shell mode vibration analysis are shown in Fig. 11. Taking the lessons learned from the previous beam mode analysis, here a white noise spectrum was added to the neutron fluxes. In the time domain flux (Fig. 11A) it is apparent that the variation was caused by a single vibration frequency. This frequency was identified as 8 Hz in the frequency domain transformation (Fig. 11B). The NCPSD (Fig. 11C) and Coherence (Fig. 11D) analyses of flux pairs showed the peak's commonality and phase difference's validity. At 8 Hz, the neighboring flux pairs were out of phase while the opposite pairs were in phase (Fig. 11E). This pattern implies that the vibration was of a single shell mode vibration at 8 Hz.

Results for beam mode vibration are shown in Fig. 12. The blue lines are the fluxes from the bottom part detectors and the red lines are from top part detectors. Similarly to the first order beam mode vibration, the vibration frequencies detected were 8 Hz and 15 Hz, which shared commonality and were coherent among detector pairs as shown in (Fig. 12B–D). The pattern of phase differences at 8 Hz indicates that the vibration was of beam mode along the x-axis. At 15 Hz, this pattern changed to suggest a beam mode

Table 1 – Vibration mode by phase differences.

Vibration mode	Phase difference	
	Adjacent	Opposite
Beam mode along x-axis	Out of phase	Out of phase
Beam mode along y-axis	In phase	Out of phase
Shell mode 45° to x- and y-axes	Out of phase	In phase

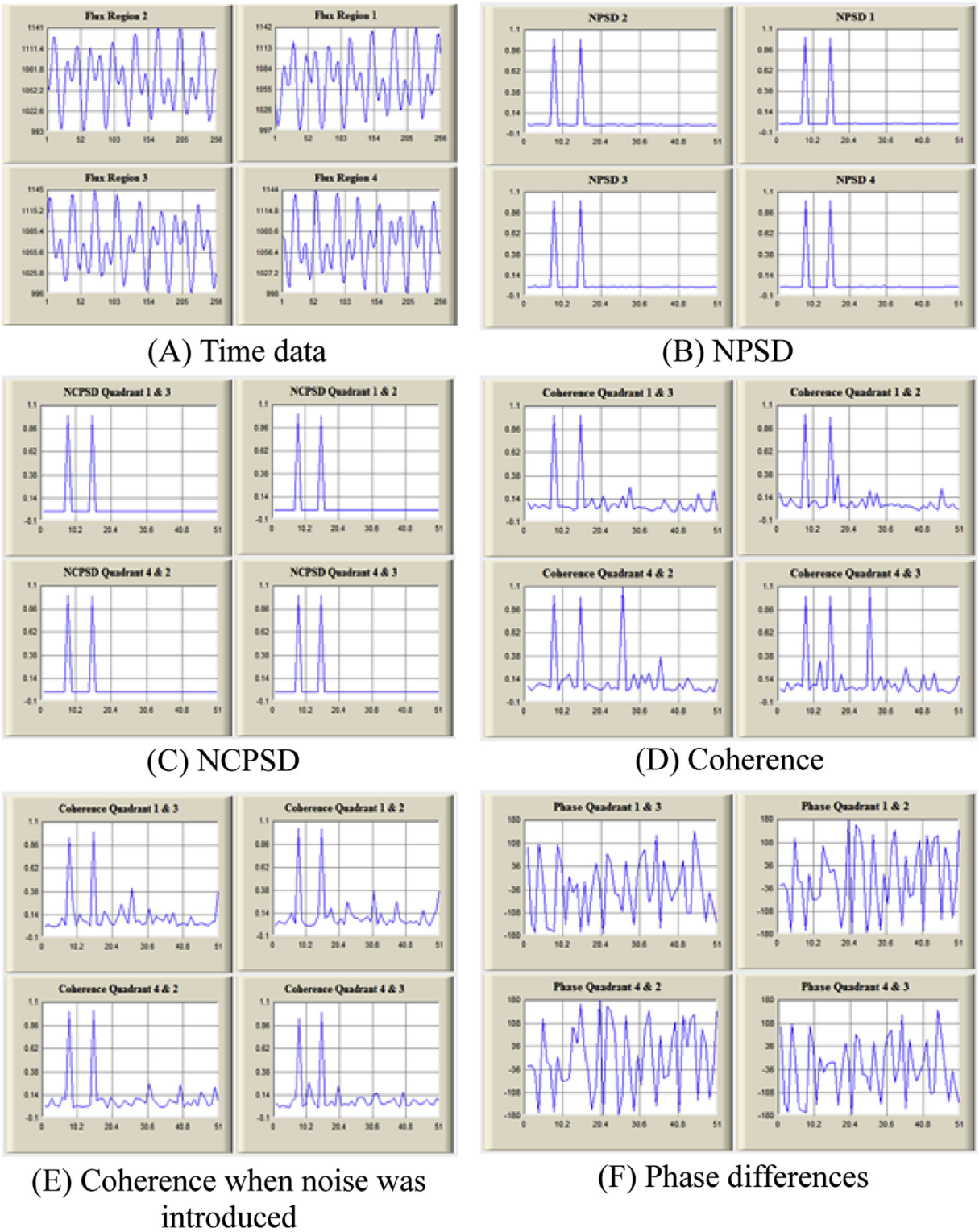

Fig. 10 – First order beam mode results. NCPSD, normalized cross power spectral density; NPSD: normalized power spectral density. Frequency domain plots were limited up to 51 Hz to give a visual clarity of detected signals. NPSD and NCPSD show frequency peaks at 8 Hz and 15 Hz. The 26 Hz peak in Coherence plots was filtered out by introducing noise into the neutron flux data. Phase diagram was expressed in degrees.

vibration along the y-axis. Furthermore, all the top part fluxes shared commonality but were out of phase with their bottom counterparts. This implies that the upper half of the CSB moved in an opposite direction to its bottom half by a phase difference of π rad, suggesting that the vibration was of the third order.

The third order shell mode vibration's results are depicted in Fig 13. As expected, the peak frequencies (Fig 13B),

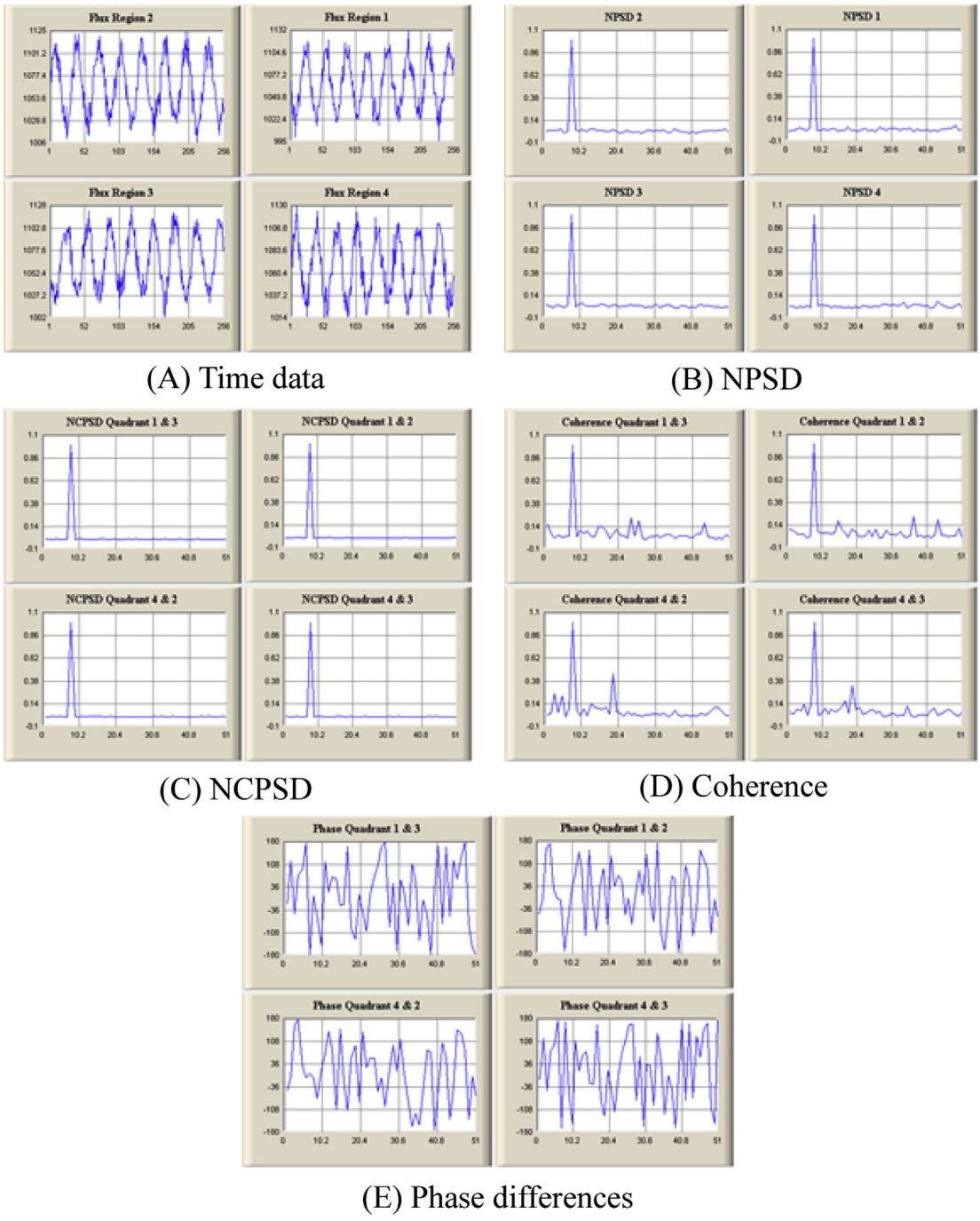

Fig. 11 – First order shell mode results. NCPSD, normalized cross power spectral density; NPSD: normalized power spectral density. The addition of noise was visualized in the time data. NPSD, NCPSD and Coherence pointed to a single peak frequency at 8 Hz.

commonality (Fig 13C), and coherence (Fig 13D) are similar to those of the first order shell mode vibration results. The phase difference between flux pairs (Fig 13E) shows an agreement with the pattern identified for the first order shell mode vibration along the $\pi/4$ rad center line. Observation of the coherence and phase differences for the 8 Hz frequency peak between the vertical detector pairs reveals that the CSB's upper section moved in the opposite direction from its lower section. This served as an indication to the third order shell mode vibration at 45° to both the x- and y-axes.

The completion time for a sequential processing simulation when executed on a quad-core central processing unit was 205,781 ms, while for a parallel processing simulation the completion time was 55,973 ms. The parallel processing method was therefore 3.7 times faster than the sequential processing. Since parallel processing was applied to the random walk only, this presumes that the ratio will approach

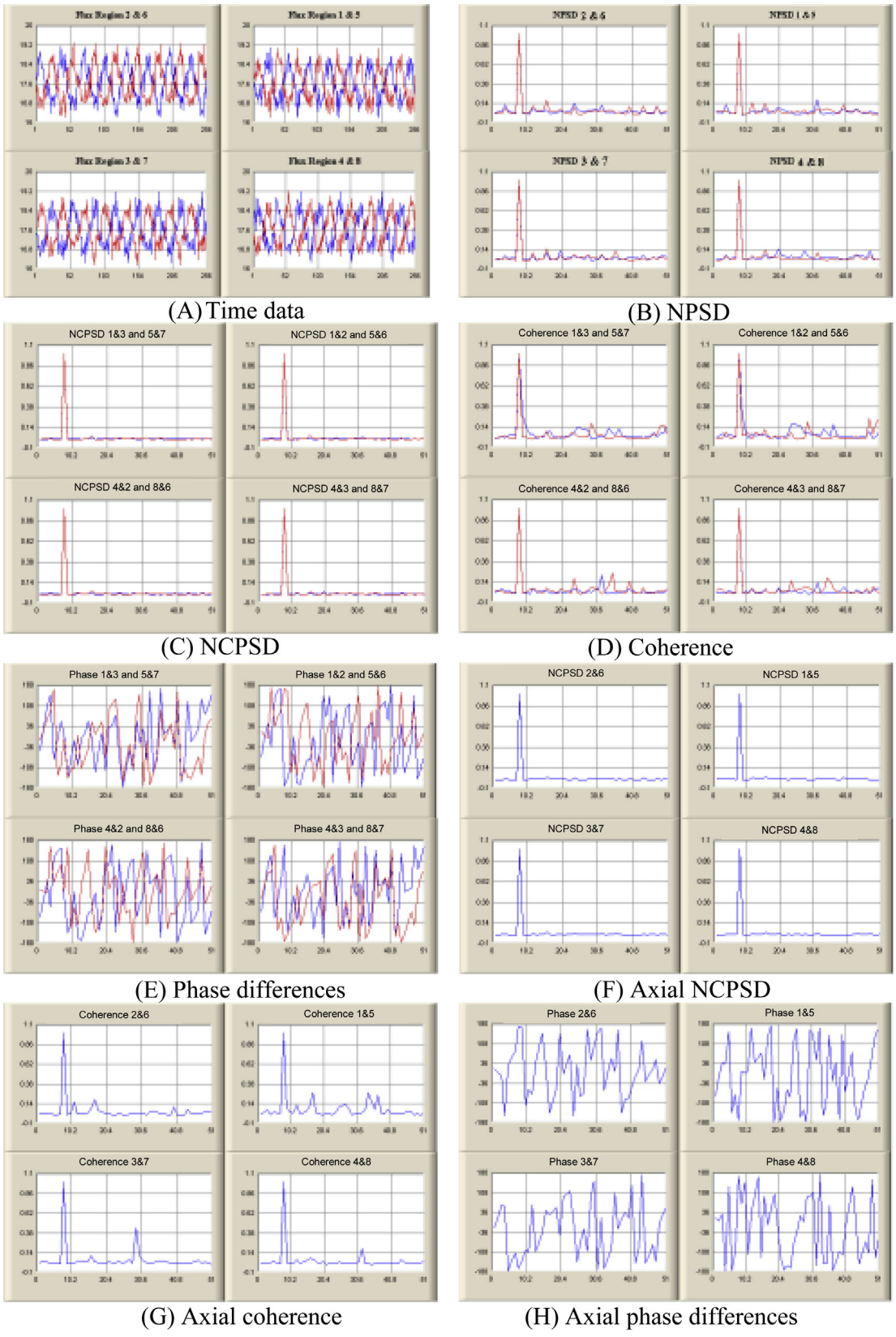

Fig. 12 – Third order beam mode vibration results. Red lines represent signals from upper section detectors while blue indicates lower section ones. Both horizontal and axial signal pairs showed a frequency peak at 8 Hz.

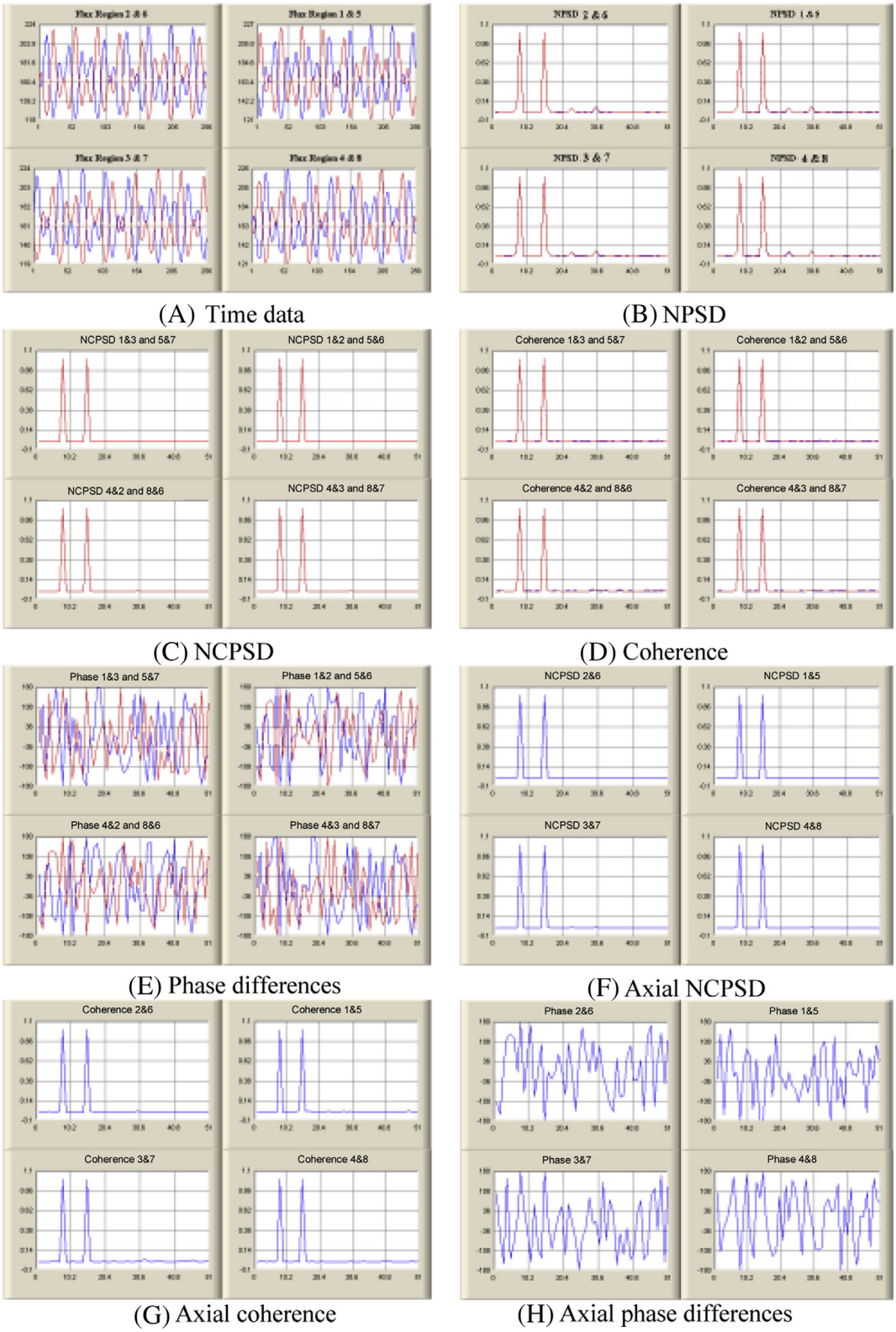

Fig. 13 – Third order shell mode vibration results. Red lines represent signals from upper section detectors while blue indicates lower section ones. Horizontal and axial signal pairs showed frequency peaks at 8 Hz and 15 Hz.

4.0 as the execution time for the random walk is significantly longer than the other processes, i.e., when the number of neutrons and batches increases.

For both the vibration modes, the FIS module successfully identified the vibration frequencies, direction, modes, and order in >0.4 ms. This allows for a real-time in-service monitoring application. Monitoring for the vibration mode, frequency, and direction might provide information on the CSB's clamping integrity. A change of the vibration order and frequency might also be associated with the condition of physical contact with snubbers at the CSB's lower end.

In conclusion, this study demonstrated the application of an NNA algorithm and a fuzzy logic decision support system to monitoring complex vibrations of a CSB under a simulated environment.

The simulation was based on a parallelized Monte Carlo neutron transport to reduce the computational time to 3.7 times faster than a serial one. In this simulation, a stream of simulated white noise was introduced to the ex-core neutron data and it was shown that the NNA algorithm can manage this irregularity well.

The NNA algorithm was modified to include correlations between vertical flux pairs. It was demonstrated that when ex-core detectors were arranged at two different elevations, the modified NNA was able to monitor high order beam and shell mode vibrations with multiple peak frequencies. A deviation from the baseline vibration mode, frequency, and direction may pinpoint degradation in a specific location at the CSB's clamp. Likewise, the condition of the CSB's contact with snubbers may be monitored from the consistency of its vibration order and frequency.

The identified signal patterns from this process were used as a basis for the construction of a fuzzy logic decision support system. This system was able to classify the CSB vibration signatures in a far shorter time compared to the conventional method of manual assessment. This renders it suitable for a real-time monitoring application in PWR-type nuclear reactors. Prior to that, however, further studies using actual measurement data are required to calibrate the fuzzy membership functions to properly decide the correct vibration frequencies, orders, types, and directions.

Conflicts of interest

All contributing authors declare no conflicts of interest.

Acknowledgments

This work is supported by the Korea Radiation Safety Foundation and the Nuclear Safety and Security Commission (130532-0113-HD130).

REFERENCES

[1] W.Y. Yun, B.J. Koh, H.C. No, Vibration monitoring of core support barrel by noise and structural analysis in ULJIN nuclear plant, J. Nucl. Sci. Technol. 27 (1990) 1058–1064.
[2] S.H. Song, M.J. Jhung, Experimental modal analysis on the core support barrel of reactor internals using a scale model, KSME Int. J. 13 (1999) 585–594.
[3] S.A. Ansari, M. Haroon, Z. Sheikh, Z. Kasmi, Detection of flow-induced vibration of reactor internals by neutron noise analysis, IEEE Trans. Nucl. Sci. 55 (2008) 1670–1677.
[4] B.T. Lubin, R. Longo, T. Hammel, Analysis of internals vibration monitoring and loose part monitoring systems data related to the St. Lucie 1 thermal shield failure, Prog. Nucl. Energy (1988) 117–126.
[5] H.G. Kang, P.H. Seong, A real time monitoring system of core support barrel vibration using FEM data and self-organizing neural networks, Nucl. Eng. Design (1995) 19–29.
[6] American Society of Mechanical Engineers, Standards and Guides for Operation and Maintenance of Nuclear Power Plants, 2007.
[7] U.S. Nuclear Regulatory Commission, Regulatory Guide 1.20: Comprehensive Vibration Assessment Program for Reactor Internals During Preoperational and Initial Startup Testing, 2007.
[8] I. Lux, L. Koblinger, Monte Carlo Particle Transport Methods: Neutron and Photon Calculations, CRC Press, Boston, 1991.
[9] J.S. Bendat, A.G. Piersol, Engineering Applications of Correlation and Spectral Analysis, Wiley-Interscience, New York, 1993.
[10] B. Dede, Mathematics of Fuzzy Sets and Fuzzy Logic, Springer, New York, 2013.